Molecular Design of Negative Differential Resistance Device through Intermolecular Interaction

Hua Geng,[†] Yibin Hu,[‡] Zhigang Shuai,*,[†] Ke Xia,[‡] Hongjun Gao,[‡] and Keqiu Chen[§]

Key Laboratory of Organic Solids, Beijing National Laboratory for Molecular Science (BNLMS), Institute of Chemistry, Chinese Academy of Sciences, 100080 Beijing, P. R. China, Institute of Physics, Chinese Academy of Sciences, 100080 Beijing, P. R. China, and Department of Physics, Hunan University, 410082 Changsha, P. R. China

Received: September 19, 2007

By applying nonequilibrium Green's functions coupled with first-principles electronic structures, we investigate the transport properties of the molecule device with a donor−acceptor molecular complex sandwiched between two electrodes. The results show that the system manifests negative differential resistance (NDR) behavior. It is found that the orbital match of molecule and electrodes as well as intermolecular charge transfer are responsible for the NDR behavior.

I. Introduction

In recent years, molecular junctions based on single molecules have attracted much attention due to their potential applications in molecular electronic devices, such as molecular switch, memory devices, or field-effect transistors. Various kinds of single molecular junctions, such as short organic molecules,[1−18] long-chain polymers,[19−20] fullerenes,[21−25] carbon nanotubes,[26−29] and so on, have been reported. Many interesting physical properties have been found in these systems. The most prominent among these is negative differential resistance (NDR) behavior, which is a very useful property in molecular electronic devices such as molecule switch. NDR have also been found in some molecular junctions, and the mechanisms have also been proposed. Chen and co-workers[30] observed the NDR behavior in a phenylene ethynylene trimer substituted by nitro and amino groups on the central ring. They suggested a possible mechanism for NDR is a two-step reduction process that modifies charge transport through the molecule. Based on density functional theory calculations, Seminario and co-workers[31] proposed that charging of the molecule followed by the localization/delocalization of molecular orbitals is the mechanism behind NDR in the trimer substituted by nitro and amino groups. However, Cornil et al.[32] found that a bias-induced alignment of the molecular orbitals can lead to NDR. Taylor et al.[33] calculated the same structure by applying the TRANSIESTA package[34] and found that the side groups play an important role in NDR. Di Ventra et al.[35] reported a full transport calculation for a single benzene ring with an NO_2 ligand. They suggested that NDR results from the rotation of the ligand, activated by temperature. By applying the elastic scattering Green's function theory approach in combination with the frontier molecular orbital theory, Luo et al.[36] have also found the NDR behavior in benzene molecule junctions with donor/acceptor substitutions and suggested that the one-electron reduction is responsible for the NDR. NDR was also observed in a self-assembled monolayer of 4-*p*-terphenylthiol molecules on the Au (111) surface measured using a platinum tip[37] and resulted from resonance between the discrete electronic levels of the molecule and the very narrow density of states around the Fermi energy of the sharp metal tip. Datta and co-workers[38] found NDR in molecules such as styrene or TEMPO on Si, and showed that the NDR effect is originated from molecular levels crossing the valence or conduction band edges, which cuts off transmission. Lu et al. also found NDR effects in Si/(organic molecule)/Si junctions.[39] Polaron coupling on a molecular wire as a mechanism for NDR was also proposed by Galperin et al.[40] Recently, Bandyopadhyay and Wakayama studied the NDR behavior in the molecular junctions of electronically different dimmers and trimers of Rose Bengal.[41] In analogy to the quantum double-dot structure, Liu et al. proposed a molecular double-dot structure of metallocenes to exhibit NDR and even hysteresis through first-principles calculation.[42] In spite of a number of theoretical and experimental studies about NDR in various kinds of molecular devices, the origin of the mechanism leading to NDR is still under intense debate.

In this article, we proposed a new molecular device structure in order to realize the NDR effect, as shown in Figure 1. A bis-ethyleneditio tetrathiafulvalene (BEDT-TTF) molecule and a tetracyanoquinodimethane (TCNQ) molecule forming a TTF-TCNQ dimer are sandwiched between two gold electrodes. The distance between two gold electrodes is 17.93 Å, and the lengths of BEDT-TTF and TCNQ molecule are 13.43 and 8.51 Å, respectively. The distance between the gold electrode and BEDT-TTF is 2.25 Å, and molecules contact with the two gold electrodes physically. Two molecules are nearly parallel, and the distance between them is about 3.00 Å.

It is known that tetrathiafulvallene (TTF) derivatives are ideally suited as components because they are reversible and stable electron donors.[43−45] In fact, the BEDT-TTF molecule acts as an electron donor molecule, and the TCNQ molecule acts as an acceptor molecule: namely, a donor−acceptor molecular complex sandwiched between two electrodes. The molecular structure can be found in ref 46. In the present work, by applying a first-principles computational method, we investigate the transport properties of the molecular junctions. The results show that NDR can be observed in such molecular device.

---

* Corresponding author. E-mail: zgshuai@iccas.ac.cn.
[†] Institute of Chemistry, Chinese Academy of Sciences.
[‡] Institute of Physics, Chinese Academy of Sciences.
[§] Hunan University.

10.1021/jp077533f CCC: $37.00

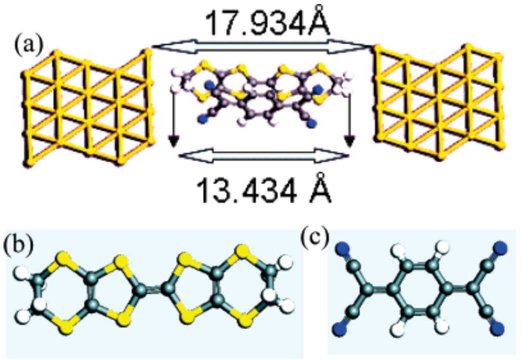

Figure 1. (a) Device model, (b) BEDT-TTF molecule, and (c) TCNQ molecule.

II. Theoretical Methodology

We use Matdcal package, developed by Guo's group,[47−48] to investigate transport properties of the TTF-TCNQ structure. Matdcal combines the Keldysh nonequilibrium Green's function (NEGF) formalism and density functional theory (DFT). The basic idea of the NEGF-DFT method is to calculate the device's electronic potential and Hamiltonian based on DFT and to populate the electronic structure using NEGF formalism. It has employed a linear combination of atomic orbital (LCAO), and chooses the fireball basis set, which is derived from the eigenfunctions of standard norm-conserving pseudopotential.[49] It uses real space numerical techniques to deal with open device boundaries. The exchange-correlation potential is treated at the local density approximation level. Matdcal is well suited to study the ballistic transport through the molecular junction.

III. Results and Discussion

We have investigated the single BEDT-TTF molecule and the TTF-TCNQ complex molecular orbital when there is no current flow through and no electrode exists. In Figure 2, we found that the HOMO−LUMO gap of the BEDT-TTF molecule is 1.31 eV, and HOMO−LUMO and HOMO−LUMO+1 gap of the TTF-TCNQ structure are 0.4 and 1.14 eV, respectively. From the figure, we can see clearly that the HOMO orbital of the TTF-TCNQ structure distributes over the entire BEDT-TTF molecule; the LUMO orbital of the TTF-TCNQ structure largely distributes over the TCNQ molecule, and the LUMO+1 orbital of the TTF-TCNQ structure almost centralizes on the BEDT-TTF molecule. Moreover, we compare the HOMO orbital of TTF-TCNQ and BEDT-TTF, we found that the HOMO orbital centralizes on the whole BEDT-TTF molecule for the TTF-TCNQ structure, whereas the HOMO orbital of the BEDT-TTF molecule centralizes on the two center rings of the BEDT-TTF molecule. The LUMO+1 orbital of TTF-TCNQ corresponds to the LUMO orbital of BEDT-TTF. These results show that there is charge transfer between BEDT-TTF and TCNQ. Such an intermolecular interaction could lead to new transport properties different from single BEDT-TTF or TCNQ molecular device.

Figure 3 shows the current through the molecule junction as a function of the bias voltage applied to the device. As we have know, the current is calculated by the Landauer−Buttiker formula:[50] $I = \int_{\mu_L}^{\mu_R} T(E,V_b)\, dE$, where $\mu_L = -eV_b$, $\mu_R = 0$, $T(E,V_b)$ is the transmission probability for electrons incident at an energy E through a device under a bias V_b. From the I−V curve, we found that there are obvious current increases at low bias, and then it becomes smooth with bias increase. When introducing the TCNQ molecule, the HLG has decreased largely from 1.31 to 0.4 eV, and the LUMO orbital is very close to the Fermi level, as we can expect that we can obtain a large current at low voltage. Figure 4a gives the transmission spectrum dependent on voltage. There are two scattering channels, corresponding to HOMO and LUMO molecular orbitals, respectively. When the molecules are in electrode environments, the HLG have decreased to about 0.1 eV. The LUMO orbital have entered the bias window at 0.2 V, so there is a large current at 0.2 volt. With an increase in the bias, there are no other orbitals or channels included, and the current keep little change, when the bias voltage reaches 1.45 and 1.8 V, the current become very large, and when the bias voltage is 1.6 V, the current decreased. NDR appears between 1.45 and 1.6 V; as the bias voltage goes higher, we got another NDR region. In the following, we will explain in detail the NDR phenomena.

To investigating the mechanism responsible for NDR, we analyze the transmission coefficient spectrums for 1.45, 1.6, and 1.8 V as shown in Figure 4. Each transmission coefficient

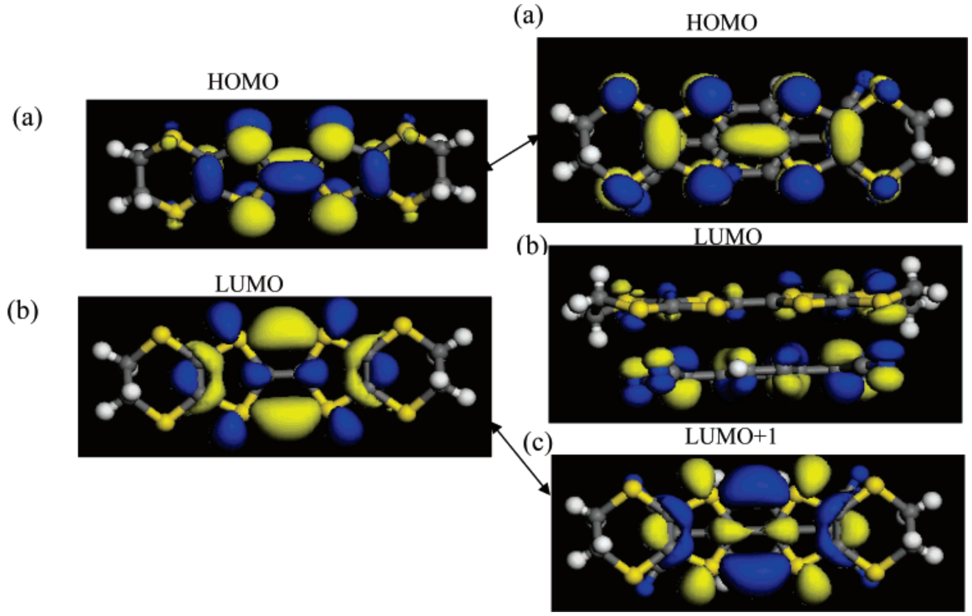

Figure 2. Comparison of molecular orbital for BEDT-TTF (left) and TTF-TCNQ structure (right), (a) HOMO, (b) LUMO, (c) LUMO+1.

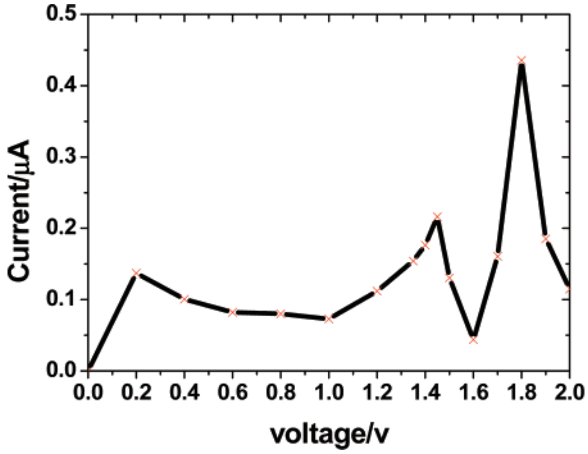

Figure 3. Calculated current−voltage characteristics of the device.

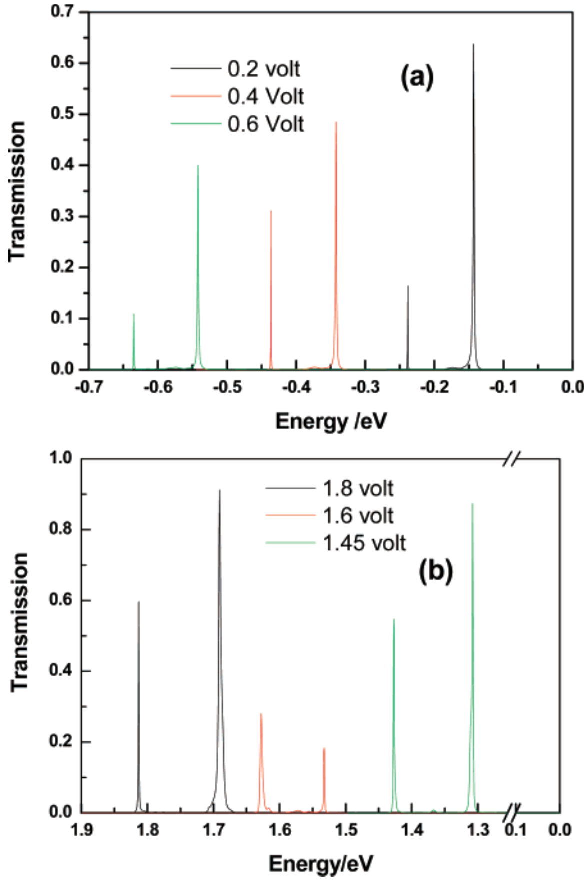

Figure 4. Transmission coefficient spectrum for bias at (a) 0.2, 0.4, and 0.6 V; (b) 1.45, 1.6, and 1.8 V.

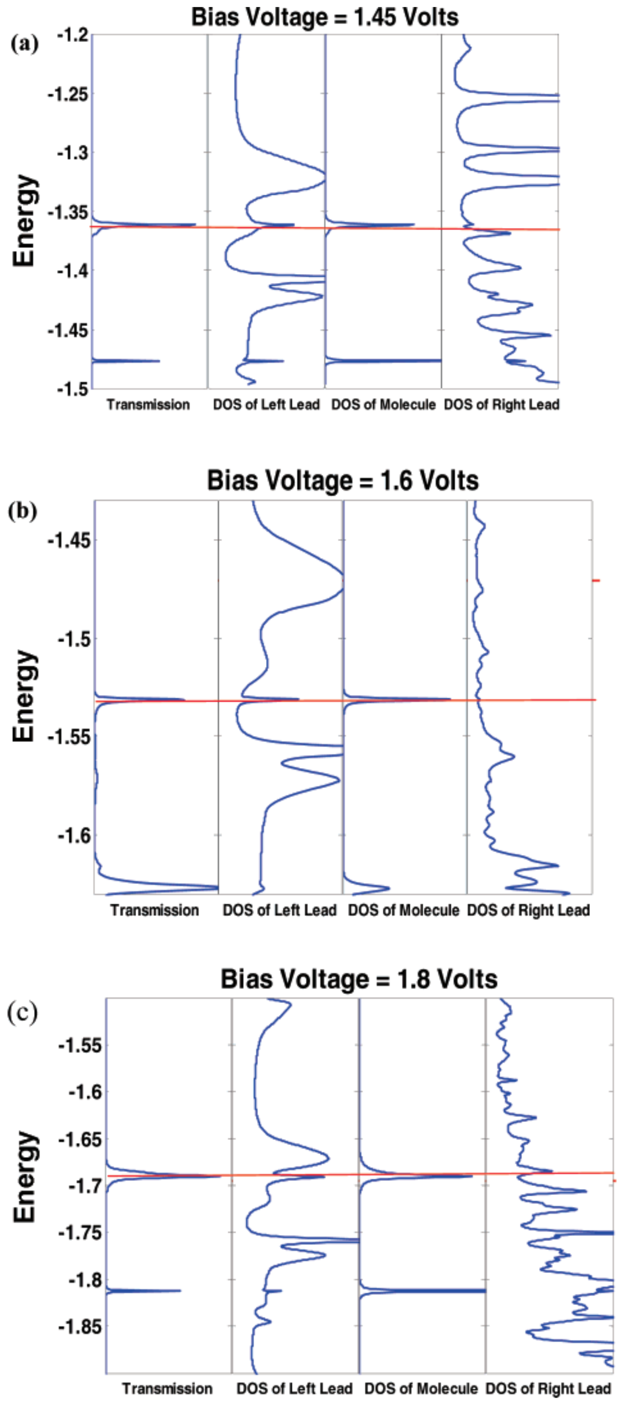

Figure 5. Comparison of the transmission with the partial DOS of the leads and the molecules at three different biases. The red lines are guide for the eye.

spectrum has two transmission peaks: one transmission peak is within the bias energy window, and the other peak is out of the bias energy window. That means that there are two scattering channels, but only one of the channels makes its contribution to current. These two scattering channels correspond to the TTF-TCNQ structure's HOMO and LUMO orbitals. In our calculation, we have set the external bias voltage (V_b) on the left gold electrode. That means that left gold electrode's chemical potential is $-eV_b$, lower than the chemical potential of the right electrode. With the increase in the bias voltage, we find that the shift of these scattering channels is almost the same as the energy shift of the left gold electrode's chemical potential due to the bias. From Figure 4, we can also see that the transmission peak for 1.6 V is much lower than the transmission peak for 1.45 and 1.8 V. In fact, this is the reason for using NDR in this device.

To find out why the transmission peak intensities change as the bias increases, we analyze the partial density of states (PDOS) of the left electrode, the right electrode, and the TTF-TCNQ structure at 1.45, 1.6, and 1.8 V, as shown in Figure 5. Note that the PDOS peaks of the TTF-TCNQ structure and its transmission peaks appear at the same energy. When we focus on the PDOS of the left electrode, we can find that there is one PDOS peak which is always located in the proximity of a TTF-TCNQ's PDOS peak. When we focus on the PDOS of the right electrode, we can find that, only when the bias voltages are at 1.45 and 1.8 V, there exists one PDOS peak very close to the

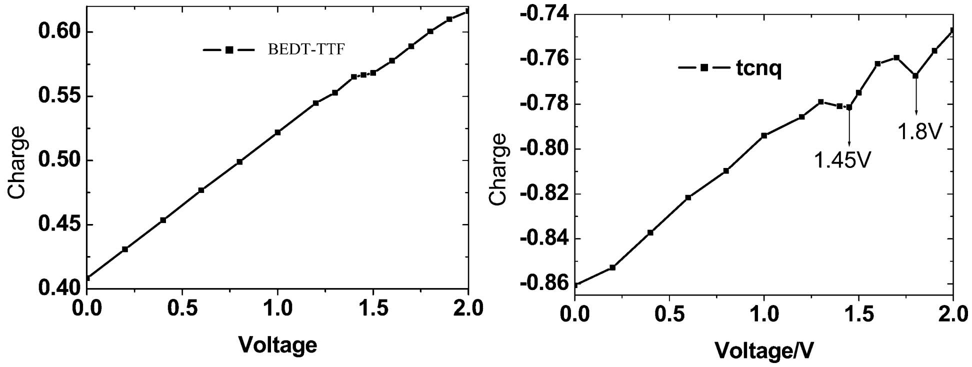

Figure 6. Dependences of Mulliken charges of BEDT-TTF and TCNQ molecules on bias voltage.

TABLE 1: Scattering Wave Function Integral at Different Bias Voltages

1.45 V		1.60 V		1.80 V	
−14.11	0.014 + 0.0023i	−45.97	0.017 + 0.00018i	−11.49	0.020 + 0.0038i
0.014−0.0023i	−0.20	0.017−0.00018i	−0.21	0.020−0.0038i	−0.66

molecule's PDOS peak, and when the bias voltage is at 1.6 V, there does not exist such closeness of PDOS peaks in energy. Thus, it can be concluded that the NDR is due to the resonance when PDOSs from different parts (left, center, and right) are matching.

In fact, in our calculations, the energy level of scattering channels is always fixed at the chemical potential of the left gold electrode, a common strategy. In this case, the wave function overlap between the center part and right electrode part plays an essential role. We then calculate the scattering wave function integral

$$\begin{pmatrix} H_{\mathrm{cc}} & H_{\mathrm{cr}} \\ H_{\mathrm{rc}} & H_{\mathrm{rr}} \end{pmatrix}$$

of the molecular device. H_{cc} is the scattering wave function integral of center part. H_{rr} is the scattering wave function integral of right electrode part. H_{cr} and H_{rc} are the scattering wave function exchange integrals between center part and right electrode part. The result is listed in Table 1 with the same ordering as the matrix form. We find that H_{cr} does not change much as the bias changes, the major modification is the diagonal elements of the hopping matrix. H_{cc} at 1.6 V is much larger than at 1.45 and 1.8 V. The wave function of the device is a linear combination of the wave function in the electrode and the center part and forming bonding and antibonding states. As the energy levels of these two parts approach each other, this linear combination is almost 50−50, and the wave function extends over the whole device. So the electrons can pass through the molecule device easily through bonding states and antibonding states when the bias voltage is 1.45 and 1.8 V.

Analysis from the Mulliken charge is consistent with the above conclusion. Figure 6 shows that the Mulliken charge of BEDT-TTF and TCNQ molecule changes with bias voltage. We find that the Mulliken charge of BEDT-TTF and TCNQ is an almost linear response to the bias voltage, but when the bias voltage is 1.45 and 1.8 V, the Mulliken charge of TCNQ has a drop. This unusual behavior is precisely related to the orbital matching shown in the PDOS (Figure 5), indicating the peculiarity of the role of the TTF-TCNQ charge-transfer complex in demonstrating the NDR switching phenomena.

IV. Conclusion

To conclude, we have demonstrated a novel molecular device structure which promise the NDR switching behavior, namely, a donor−acceptor complex, specifically, TTF-TCNQ, through first-principles calculation coupled with nonequilibrium Green's function formalism. It is shown that the transmission spectra are dependent on the bias, and at 1.45 and 1.8 V, there occur strong resonant increases in amplitude due to the orbital matchings bewteen the molecule and the electrodes. Mulliken charge analysis indicates that the orbital resonance correlates well with intermolecular charge transfer upon applied bias voltage.

Acknowledgment. The authors are indebted to Professor Hong Guo of McGill University for providing his Matdcal programme source codes. This work is supported by the Ministry of Science and Technology of China (Grant No. 2006CB806200 and 2006CB0N0100) and NSFC (Grant No. 10425420, 20433070, and 90503013), as well as the Chinese Academy of Sciences.

References and Notes

(1) Mujica, V.; Kemp, M.; Ratner, M. A. *J. Chem. Phys.* **1994**, *101*, 6849.
(2) Lang, N. D. *Phys. Rev. B* **1995**, *52*, 5335.
(3) Samanta, M. P.; Tian, W.; Datta, S.; Henderson, J. I.; Kubiak, C. P. *Phys. Rev. B* **1996**, *53*, R7626.
(4) Reed, M. A.; Zhou, C.; Muller, C. J.; Burgin, T. P.; Tour, J. M. *Science* **1997**, *278*, 252.
(5) Datta, S.; Tian, W.; Hong, S. H.; Reifenberger, R.; Henderson, J. I.; Kubiak, C. P. *Phys. Rev. Lett.* **1997**, *79*, 2530.
(6) Yaliraki, S. N.; Ratner, M. A. *J. Chem. Phys.* **1998**, *109*, 5036.
(7) Chen, J.; Reed, M. A.; Rawlett, A. M.; Tour, J. M. *Science* **1999**, *286*, 1550.
(8) Di Ventra, M.; Pantelides, S. T.; Lang, N. D. *Appl. Phys. Lett.* **2000**, *76*, 3448.
(9) Taylor, J.; Guo, H.; Wang, J. *Phys. Rev. B* **2001**, *63*, 245407.
(10) Brandbyge, M.; Mozos, J. L.; Ordejon, P.; Taylor, J.; Stokbro, K. *Phys. Rev. B* **2002**, *65*, 165401.
(11) Lang, N. D.; Avouris, P. *Phys. Rev. B* **2001**, *64*, 125323.
(12) Wang, C. K.; Fu, Y.; Luo, Y. *Phys. Chem. Chem. Phys.* **2001**, *3*, 5017.
(13) Xue, Y.; Datta, S.; Ratner, M. A. *Chem. Phys.* **2002**, *281*, 151.
(14) Reichert, J.; Ochs, R.; Beckmann, D.; Weber, H. B.; Mayor, M.; Lohneysen, H. V. *Phys. Rev. Lett.* **2002**, *88*, 176804 .
(15) Xu, B.; Tao, N. J. *Science* **2003**, *301*, 121.
(16) Stokbro, K.; Taylor, J.; Brandbyge, M. *J. Am. Chem. Soc.* **2003**, *125*, 3674.
(17) Ke, S. H.; Baranger, H. U.; Yang, W. *J. Am. Chem. Soc.* **2004**, *126*, 15897.
(18) Tarakeshwar, P.; Palacios, J. J.; Kim, D. M. *J. Phys. Chem. B* **2006**, *110*, 7456.
(19) Hu, W.; Nakashima, H.; Furukawa, K.; Kashimura, Y.; Ajito, K.; Torimitsu, K. *Appl. Phys. Lett.* **2004**, *85*, 115 .

(20) Hu, W.; Jiang, J.; Nakashima, H.; Luo, Y.; Kashimura, Y.; Chen, K. Q.; Shuai, Z.; Furukawa, K.; Lu, W.; Liu, Y.; Zhu, D.; Torimitsu, K. *Phys. Rev. Lett.* **2006**, *96*, 27801.

(21) Park, H.; Park, J.; Lim, A. K. L.; Anderson, E. H.; Alivisatos, A. P.; Mceuen, P. L. *Nature* **2000**, *407*, 57.

(22) Park, H. K.; Park, J. W.; Lim, K. L.; Anderson, A.; Erik, H.; Alivisatos, A. P.; McEuen, P. L. *Nature* **2000**, *407*, 57.

(23) Taylor, J.; Guo, H.; Wang, J. *Phys. Rev. B* **2001**, *63*, 121104.

(24) Kaun, C. C.; Seideman, T. *Phys. Rev. Lett.* **2005**, *94*, 226801.

(25) Zhao, J.; Zeng, C. G.; Cheng, X.; Wang, K. D.; Wang, G. W.; Yang, J. L.; Hou, J. G.; Zhu, Q. S. *Phys. Rev. Lett.* **2005**, *95*, 45502.

(26) Tans, S. J.; Verschueren, A. R. M.; Dekker, C. *Nature* **1999**, *393*, 49.

(27) Yao, Z.; Postma, H. W. C.; Balents, L.; Dekker, C. *Nature* **1999**, *402*, 273.

(28) Minot, E. D.; Yaish, Y.; Sazonova, V.; Park, J. Y.; Brink, M.; McEuen, P. L. *Phys. Rev. Lett.* **2003**, *90*, 156401.

(29) Li, X. F.; Chen, K. Q.; Wang, L. L.; Long, M. Q.; Zou, B. S.; Shuai, Z. *J. Appl. Phys.* **2007**, *101*, 64514.

(30) Chen, J.; Reed, M. A.; Rawlett, A. M.; Tour, J. M. *Science* **1999**, *286*, 1550.

(31) Seminario, J. M.; Zacarias, A. G.; Tour, J. M. *J. Am. Chem. Soc.* **2000**, *122*, 3015.

(32) Cornil, J.; Karzazi, Y.; Bredas, J. L. *J. Am. Chem. Soc.* **2002**, *124*, 3516.

(33) Taylor, J.; Brandbyge, M.; Stokbro, K. *Phys. Rev. B* **2003**, *68*, 121101 (R).

(34) Brandbyge, M.; Mozos, J. L.; Ordejon, P.; Tayor, J.; Stokbro, K. *Phys. Rev. B* **2002**, *65*, 165401.

(35) Di Ventra, M.; Kim, S. G.; Pantelides, S. T.; Lang, N. D. *Phys. Rev. Lett.* **2001**, *86*, 288.

(36) Luo, Y.; Fu, Y. *J. Chem. Phys.* **2002**, *117*, 10283.

(37) Xue, Y.; Datta, S.; Hong, S. H.; Reifenberger, R.; Henderson, J. I.; Kubiak, C. P. *Phys. Rev. B* **1999**, *59*, 7852 (R).

(38) Rakshit, T.; Liang, G. C.; Ghosh, A. W.; Datta, S. *Nano Lett.* **2004**, *4*, 1803.

(39) Lu, W. C.; Meunier, V.; Bernholc, J. *Phys. Rev. Lett.* **2005**, *95*, 206805.

(40) Galperin, M.; Ratner, M. A.; Nitzan, A. *Nano Lett.* **2005**, *5*, 125.

(41) Bandyopadhyay, A.; Wakayama, Y. *Appl. Phys. Lett.* **2007**, *90*, 23512.

(42) Liu, R.; Ke, S. H.; Baranger, H. U.; Yang, W. T. *J. Am. Chem. Soc.* **2006**, *128*, 6274

(43) Nielsen, M. B.; Lomholt, C.; Becher, J. *Chem. Soc. Rev.* **2000**, *29*, 153.

(44) Segura, J. L.; Martin, N. *Angew. Chem., Int. Ed.* **2001**, *40*, 1372.

(45) Gomar-Nadal, E.; Ramachandran, G. K.; Chen, F.; Burgin, T.; Rovira, C.; Amabilino, D. B.; Lindsay, S. M. *J. Phys. Chem. B* **2004**, *108*, 7213.

(46) Hasegawa, T.; Inukai, K.; Kagoshima, S.; Sugawara, T.; Mochida, T.; Sugiura, S.; Iwasa, Y. *Chem. Comm.* **1997**, 1377.

(47) Taylor, J. Ph.D. Thesis; McGill University: Toronto, Canada.

(48) Taylor, J.; Guo, H.; Wang, J. *Phys. Rev. B* **2001**, *63*, 245407.

(49) Soler, J. M.; Artacho, E.; Gale, J. D.; García, A.; Junquera, J.; Ordejón P.; Sánchez-Portal, D. *J. Phys. Condens. Matter* **2002**, *14*, 2745.

(50) (a) Büttiker, M.; Imry, Y.; Landauer, T.; Pinhas, S. *Phys. Rev. B* **1985**, *31*, 6207. (b) Büttiker, M. *Phys. Rev. Lett.* **1986**, *57*, 1761. (c) *IBM J. Rev. Dev.* **1988**, *32*, 317. (d) *Phys. Rev. B* **1988**, *38*, 9375.